

Supporting Information

Time-Resolved Luminescence Detection of Syk Kinase Activity Through Terbium-Sensitization

Andrew M. Lipchik and Laurie L. Parker

Department of Medicinal Chemistry and Molecular Pharmacology, Purdue Center for
Cancer Research, Purdue University, 201 S. University Street, West Lafayette, IN 47907

Optimal luminescence excitation of SAS tide and pSAS tide Tb³⁺ complexes

The UV absorbance spectra of the peptide biosensor in its phosphorylated and unphosphorylated form both displayed a single absorbance band. The unphosphorylated form, SAS tide, displayed maximum absorption at 275 nm, whereas the maximum absorbance shifted to 266 nm for the phosphorylated form, pSAS tide (Figure S1A). These absorbance bands did not shift in the presence of Tb³⁺ (Figure S1B). This shift in the maximum UV absorbance offered an additional advantage for the detection of the phosphorylated form over the unphosphorylated form of the biosensor. Using a monochromator, the excitation source can be filtered to a single wavelength, allowing for specific excitation of a particular chromophore and preferred detection of a particular form of the peptide. The differences in luminescent signal obtained from excitation of each species via either maximum absorption wavelength were characterized. Solutions containing SAS tide:Tb³⁺ and pSAS tide:Tb³⁺ complexes were excited at 266 nm and 275 nm and the luminescent emission spectra were collected. SAS tide:Tb³⁺ excitation with each wavelength resulted in similar emission spectra; however, the area under the spectra decreased by 16% when 266 nm was used as the excitation wavelength compared to 275 nm (Figure S1C). Similarly, when the pSAS tide:Tb³⁺ complex was excited with 275 nm compared to 266 nm the emission area under the emission spectra decreased by 32% (Figure S1D).

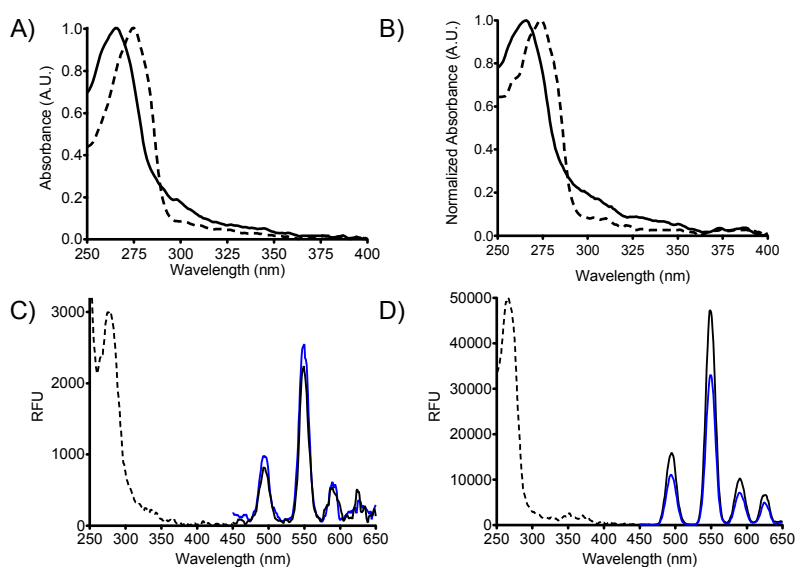


Figure S1. Absorption and luminescent properties of SAS tide and pSAS tide. **A)** UV-Vis spectra of SAS tide (---) and pSAS tide (—) without Tb³⁺. **B)** UV-Vis spectra of SAS tide (---) and pSAS tide (—) in the presence of Tb³⁺. Luminescence excitation (---) and emission spectra with 266 nm_{Ex} (—, black) and at 275 nm_{Ex} (—, blue) for SAS tide:Tb³⁺ (**C**) and pSAS tide:Tb³⁺ (**D**) complexes. Luminescence emission spectra were collected from 15 μM peptide in the presence of 100 μM Tb³⁺, 10 mM HEPES, 100 mM NaCl with a 50 μs delay and 1 ms collection time. Each spectrum represents that average of three replicates.

Terbium complexation with SAStide and pSASTide

Luminescence emission spectra were collected of SAStide or pSASTide in the presence of varying concentrations of terbium. The integrated emission spectral area was normalized to plateau of the first hyperbolic curve. The addition of terbium to both peptides resulted in a hyperbolic increase in terbium-sensitized luminescence characteristic of one site binding (the model for which is further described in the main text). The addition of terbium beyond 50 μM (50 equivalents) to SAStide or pSASTide resulted in increased terbium sensitized luminescence with an inflection and plateau (respectively) at approximately quantized ratios of two- and three- fold greater than the 1:1 complex plateau. Since terbium sensitized luminescence is proportional to the amount of terbium bound in the complex, it is reasonable to interpret that the 2 and 3 fold increase in luminescence corresponds to the formation of the 1:2 and 1:3 pSASTide:Tb³⁺ complexes and the 1:2 SAStide:Tb³⁺ complex. This is further supported by data from electrospray ionization mass spectrometry analysis, which indicates adducts of 1, 2 and 3 Tb³⁺ ions associated with the phosphorylated SAStide peptide (and even also exhibited 1:3 complexation of the unphosphorylated species with Tb³⁺) (Fig. S3).

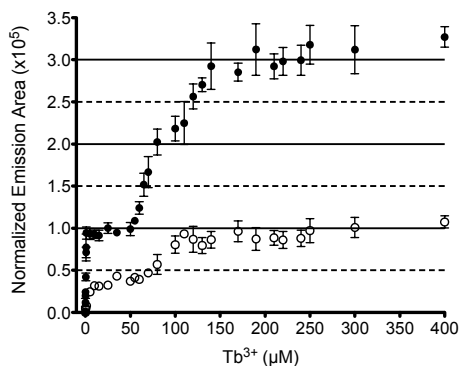


Figure S2. Terbium binding to SAStide and pSASTide. Spectra were collected from 1 μM pSASTide (●) or SAStide (○) in the presence of varying concentrations of Tb³⁺ in 10mM HEPES, 100mM NaCl, pH 7.5, $\lambda_{\text{ex}} = 266$ nm for pSASTide and $\lambda_{\text{ex}} = 275$ nm for SAStide, 1000ms collection time, 50 μsec delay time and sensitivity 180. Data represent averages \pm SEM of experiment performed in triplicate.

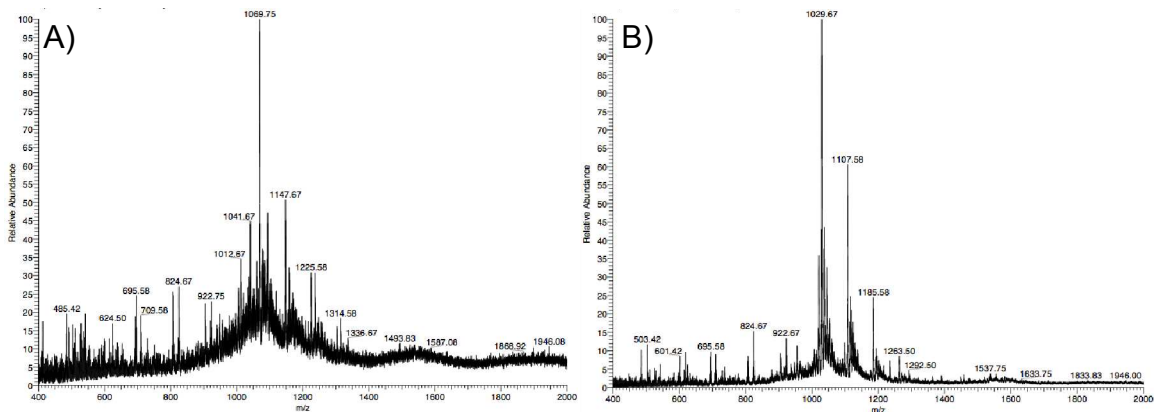


Figure S3. Electrospray ionization mass spectrometric detection of terbium binding to SAStide and pSAStide. Negative mode ESI mass spectra of 15 μM pSAStide (A) or SAStide (B) peptides in the presence of 100 μM Tb^{3+} . pSAStide displays the formation of 1:1, 2:1 and 3:1 Tb^{3+} :pSAStide and Tb^{3+} :SAStide complexes.

Determination of pSAStide: Tb^{3+} hydration number

Luminescence emission spectra were collected on a Biotek Synergy4 plate reader at 23°C in black 384-well plates (Greiner Fluortrac 200). Spectra were collected from 450-650 nm after excitation at 266 nm with a delay time starting at 100 μsec , increasing in steps of 100 μsec to 5000 μsec , and a collection time of 1 ms. Samples were prepared with 1 μM pSAStide or SAStide with 1 μM Tb^{3+} in 100 mM NaCl, 10 mM HEPES pH 7.5 with varying percentages of D_2O in 50 μL total volume. The intensity of the emission peak at 549 nm was used as the metric for luminescence lifetime. Data were fitted to a single exponential decay curve using GraphPad Prism and lifetimes in varying percentages of D_2O were determined and plotted against the mole fraction of H_2O . (Figure S2) The luminescent decay rate of pSAStide: Tb^{3+} and SAStide: Tb^{3+} in D_2O were interpolated from this plot and applied to the following equation (S1):

$$q = A'(k_{\text{H}_2\text{O}} - k_{\text{D}_2\text{O}} - 0.06) \quad (\text{S1})$$

where $k_{\text{H}_2\text{O}}$ is the luminescence decay constant in H_2O and $k_{\text{D}_2\text{O}}$ is the luminescence decay constant in D_2O extrapolated from the plot. A' is the lanthanide specific constant, which is 5 for Tb^{3+} . The decay rates were 2.02 and 2.44 in H_2O and D_2O respectively for pSAStide: Tb^{3+} . These data produced a q value of 0.12 indicating that the hydration number of the pSAStide: Tb^{3+} complex is approximately 0. The SAStide: Tb^{3+} complex displayed luminescence decay rates of 1.88 and 2.92 in H_2O and D_2O respectively. These data in equation S1 gave a q value of 0.66 indicating 1 water molecule in the coordination sphere.

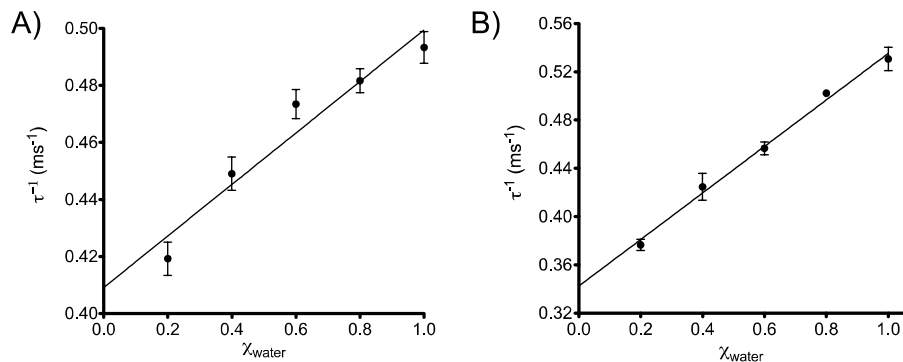


Figure S4. Luminescence decay rates with increasing mole fraction of H₂O of pSAS tide:Tb³⁺ (A) and SAS tide:Tb³⁺ (B). Extrapolation to a H₂O-free solution provides the rate constant in D₂O. Data represent the average \pm SEM of three individual replicates.

Determination of pSAS tide:Tb³⁺ quantum yield

The quantum yield of the pSAS tide:Tb³⁺ complex was determined using diffusion-enhanced energy transfer between the pSAS tide:Tb³⁺ complex and FITC. The pSAS tide:Tb³⁺ complex (4 μ M pSAS tide and 10 μ M Tb³⁺) was mixed with various concentrations of the fluorescent acceptor, FITC, which was used as a standard to compare excited-state lifetimes and intensities of emission. Luminescence decay spectra were collected with increasing delay times and spectra were normalized to the emission at 495 nm. The area under the emission spectra was integrated. The lifetime of pSAS tide:Tb³⁺ was 0.43 ms and decreased to 0.37 ms (15% energy transfer) in the presence of 2 μ M FITC, 0.34 ms (21% energy transfer) in 4 μ M FITC and 0.28 ms (36% energy transfer) in 8 μ M FITC. It was observed that increasing the concentration of FITC decreased the lifetime while increasing the energy transfer (indicated by the increase in the intensity of the FITC emission peak at 520 nm). The quantum yield was determined using this information in the equation below where Q_a is the quantum yield of FITC at pH 7.5, I_{da} is the area under the curve for the luminescence spectrum of the pSAS tide:Tb³⁺ complex in the absence of FITC, I_{ad} is the difference in area under the curve for the luminescence spectrum for the pSAS tide:Tb³⁺ in the absence vs. the presence of FITC, τ_d is the excited-state lifetime of the donor (pSAS tide:Tb³⁺) luminescence, τ_{da} is the excited-state lifetime of the donor in the presence of the acceptor (pSAS tide:Tb³⁺ in the presence of FITC)

$$Q_{Ln} = Q_a * I_{da} * (\tau_d - \tau_{ad}) / (I_{ad} * \tau_{ad}) \quad (S2)$$

The quantum yields in the presence of 2 μ M, 4 μ M and 8 μ M FITC were determined to be 0.36, 0.35, and 0.32 respectively for an average quantum yield of 0.34.

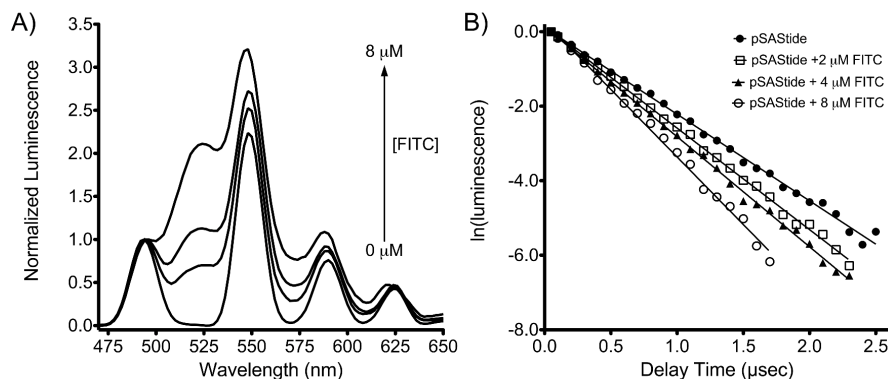


Figure S5. Determination of pSASTide-Tb³⁺ quantum yield A) Emission spectra of pSASTide-Tb³⁺ complex in the presence of various concentrations of FITC. B) Luminescence decay plots of the pSASTide:Tb³⁺ in the presence of various concentrations of FITC.

pSASTide:Tb³⁺ signal stability and resistance to interference

The effect of various buffer components on the luminescence of the pSASTide:Tb³⁺ and SASTide:Tb³⁺ complexes were assessed individually and compared to their luminescence in the absence of interference. Samples were prepared, TR-luminescence spectra were collected in triplicate as described before and the areas under the curves were determined. Most components displayed minimal interference, with the exception of those containing hard bases such as the phosphate groups of ATP, the sulfoxide group of DMSO, and the oxoanion of pervanadate. These components produced increased signal from the unphosphorylated sample and slightly decreased signal from the phosphorylated sample, resulting in the potential for a net, albeit not severe or limiting, decrease in signal to noise (as discussed in the main text).

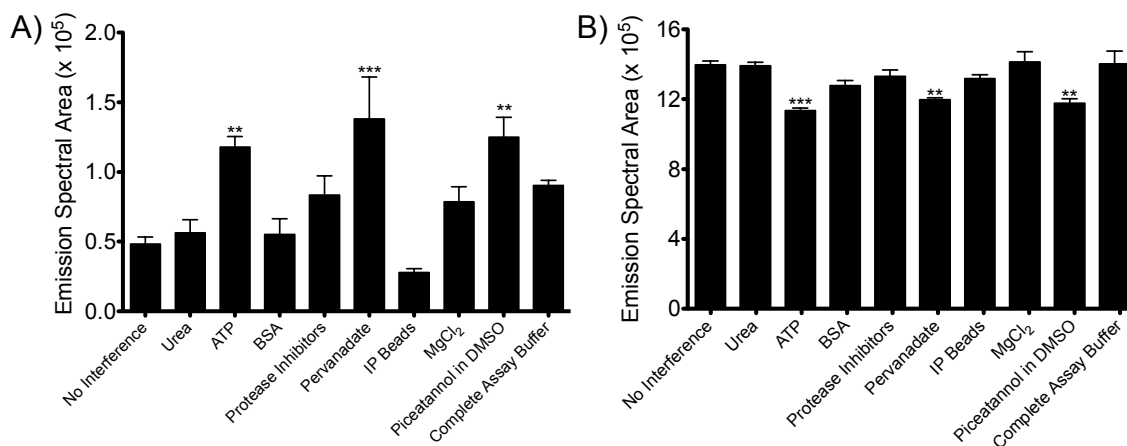


Figure S6. pSASTide:Tb³⁺ and SASTide:Tb³⁺ luminescence interference from assay components. TR-luminescence measurements were performed for the negative control SASTide (15 μM) (A) or the positive control pSASTide (15 μM) (B) in the presence of 100 μM Tb³⁺, 100 mM NaCl, 10 mM HEPES pH 7.5 and the components comprising the *in vitro* kinase assay. 2.4 M Urea, 4 mM MgCl₂, 40 μM ATP, 0.4 μM

prevanidate, 0.04 $\mu\text{g}/\mu\text{L}$ aprotinin and leupeptin, 50 $\text{ng}/\mu\text{L}$ BSA, 2% DMSO, 100 μM piceannatol. Data were analyzed using repeated measures one-way ANOVA with a Dunnett post-test using the no interference sample as the control for both SAS tide and pSAS tide. Statistical significance is indicated as follows: * $P < 0.05$, ** $P < 0.01$, *** $P < 0.001$.

Table S1. *In vitro* assay components and change on luminescence signal

Component	Concentration	pSAS tide:Tb ³⁺ Average Area ($\times 10^5$)	pSAS tide:Tb ³⁺ Percent Change (\pm SEM)	SAS tide:Tb ³⁺ Average Area ($\times 10^5$)	SAS tide:Tb ³⁺ Percent Change (\pm SEM)
Urea	2.4 M	13.61	-2.04 \pm 0.80	0.56	+121.29 \pm 49.21
BSA	50 $\text{ng}/\mu\text{L}$	12.62	-8.46 \pm 5.68	0.55	+112.33 \pm 18.29
MgCl ₂	4 mM	13.96	+1.01 \pm 5.24	0.79	+161.71 \pm 11.22
Protease Inhibitors	0.1 $\mu\text{g}/\mu\text{L}$ Aprotinin 0.1 $\mu\text{g}/\mu\text{L}$ Leupeptin	13.14	-4.77 \pm 2.19	0.83	+171.09 \pm 27.23
ATP	40 μM	11.20	-18.82 \pm 2.47	1.18	+249.78 \pm 54.96
Pervanadate	0.4 μM	11.82	-14.28 \pm 2.77	1.38	+279.91 \pm 54.32
Piceatannol and DMSO	100 μM Piceatannol 2% DMSO	11.62	-15.81 \pm 1.08	1.22	+121.75 \pm 23.27
IP Beads	1:25 dilution	13.01	-5.72 \pm 2.05	0.28	-59.41 \pm 18.72
Assay Buffer		13.84	-5.62 \pm 4.97	0.90	+189.71 \pm 24.69

A number of buffers are commonly used in biological assays, including phosphate buffers and buffers containing other hard base moieties that could potentially compete for Tb³⁺ binding and interfere with the luminescence of the biosensor. The luminescence of the pSAS tide:Tb³⁺ complex was measured in the presence of 4(2-hydroxyethyl)-1-piperzaineethanesulfonic acid (HEPES), 2-(N-morpholino)ethanesulfonic acid (MES), 3-(N-morpholine)propanesulfonic acid (MOPS), phosphate and tris(hydroxymethyl)aminomethane (Tris) buffers at various concentrations (1 μM – 70 mM). The luminescence emission spectra of pSAS tide:Tb³⁺ were robust for HEPES, MES, MOPS and Tris over all concentrations with only a small decrease in signal at higher concentrations (70 mM). In the presence of the phosphate buffer (from 1 μM to 1 mM) luminescence emission spectra were robust but significantly diminished. At concentrations greater than 1 mM the robustness of the spectra was lost.

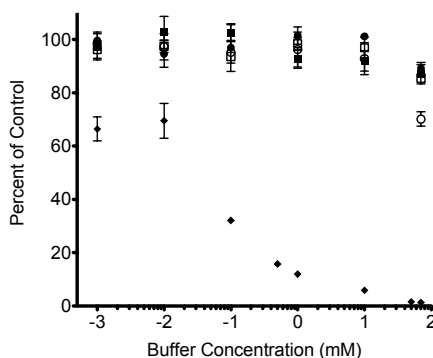


Figure S7. Compatibility of pSASTide:Tb³⁺ assay with biological buffers. Luminescent emission spectra of 15 μM pSASTide in the presence of 100 μM of Tb³⁺, 100 mM NaCl and various buffers including HEPES (●), MES (○), MOPS (□), Phosphate (◆) and Tris (◻) at pH 7.5. Spectra were collected in triplicate and the area of each spectrum was calculated and taken as the percent of the no buffer control. Data represent the averages \pm SEM.

As demonstrated above phosphate can influence the signal of the pSASTide:Tb³⁺ complex by decreasing the signal and robustness of the emission spectrum (likely because of competition for binding of Tb³⁺). One of the essential cofactors required for phosphorylation is the phosphate source adenosine triphosphate, ATP. The luminescence of the pSASTide:Tb³⁺ complex was measured in presences of various concentrations of ATP. The area under each spectrum was calculated and normalized to the percent of the control in the absence of ATP. The luminescent intensity of the pSASTide:Tb³⁺ decreased in a concentration dependent manner in the presence of ATP with an approximate $K_i = 58 \mu\text{M}$. These parameters should be taken into account when designing assay and quenching conditions for Tb³⁺-based detection.

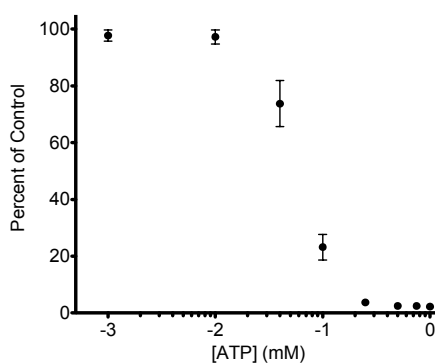


Figure S8. The influence of ATP on pSASTide:Tb³⁺ luminescence. Luminescence emission spectra of pSASTide (15 μM) in the presence of 100 μM Tb³⁺, 100 mM NaCl, 10 mM HEPES pH 7.5 and various concentrations of ATP ranging from 1 μM to 100 mM. Spectra were collected in triplicate and the area of each spectrum was calculated and taken as the percent of the control (absence of ATP). Data represent the mean \pm SEM.

Validation of SASTide phosphorylation *in vitro*

Phosphorylated SASTide was detected using a chemifluorescent ELISA-based assay in which the quenched reaction mixture was incubated in a 96-well neutravidin coated-plate to allow for affinity capture of the biotinylated substrate. The total amount of peptide in the quenched reaction mixture applied to each well was 37.5 pmol, which ensured that each well was saturated with peptide (15 pmol binding capacity) for analysis. The captured peptide was then incubated an anti-phosphotyrosine primary antibody (4G10) followed by a horseradish peroxidase-conjugated secondary antibody. Chemifluorescent detection was

accomplished by incubating each well with Amplex Red reagent and hydrogen peroxide in phosphate buffer, which gave a fluorescent signal proportional to the amount of horseradish peroxidase-conjugate antibody in each well, and thus reports the degree of phosphotyrosine present. As seen in the with the Tb³⁺ based detection, the ELISA-based assay displayed increasing fluorescent signal over time, demonstrating that SASTide was phosphorylated by Syk *in vitro*.

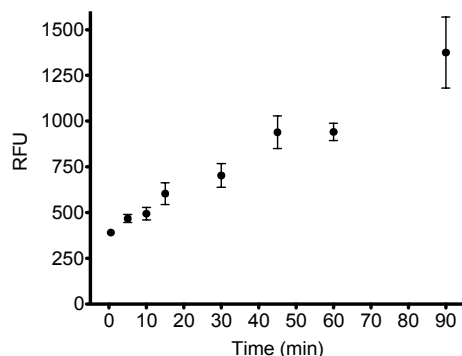


Figure S9. Validation of *in vitro* phosphorylation of SASTide using ELISA-based chemifluorescence.

The SASTide biosensor was incubated with Syk-EGFP in an *in vitro* kinase assay as described in the main text. Aliquots were removed at designated time points, quenched with EDTA and the amount of phosphorylated substrate was measured using ELISA-based detection.

Table S2. HTS assay parameters for controls

Percent Phosphorylation	CV (%)	Average (Area 10 ⁵)	Standard Deviation	Z factor	Signal Window
0%	4.21	0.90	0.07	N/A	N/A
20%	9.88	3.54	0.61	0.56	4.21
40%	9.91	5.04	0.86	0.61	5.06
60%	5.62	7.82	0.76	0.79	12.49
80%	8.78	11.03	1.68	0.70	7.32
100%	5.25	13.83	1.26	0.82	14.64

Table S3. HTS assay parameters for piceatannol dose-response inhibition of Syk

Concentration (piceatannol)	CV (%)	Average (% Activity)	Standard Deviation	Z factor	Signal Window
10 nM	12.33	114.22	24.39	0.60	4.73
100 nM	14.39	115.48	28.78	0.53	3.62
1 μM	9.86	132.41	22.61	0.68	6.73
10 μM	10.59	119.12	21.85	0.65	6.01
50 μM	7.94	101.65	13.99	0.73	8.92
100 μM	5.90	70.30	7.19	0.78	12.64
500 μM	10.63	37.53	6.91	0.58	5.04
1 mM	212.93	5.33	19.67	-13.15	-3.01
10 mM	32.59	2.74	1.54	N/A	N/A